Surface & Coatings Technology 228 (2013) 195–200

Contents lists available at SciVerse ScienceDirect

Surface & Coatings Technology

journal homepage: www.elsevier.com/locate/surfcoat

Effects of high temperature plasma immersion ion implantation on wear resistance of Ti-Si-B sintered alloys

Bruno Bacci Fernandes [a,*], Rogério Moraes Oliveira [a], Mário Ueda [a], Samantha de Fátima Magalhães Mariano [a,b], Alfeu Saraiva Ramos [c], Maxson Souza Vieira [a], Francisco Cristóvão Lourenço de Melo [d], Guilherme de Oliveira [a,b]

[a] Instituto Nacional de Pesquisas Espaciais, LAP/INPE, Av. dos Astronautas 1758, Caixa Postal 515, São José dos Campos, SP, Brazil
[b] ETEP Faculdades, Av. Barão do Rio Branco, Caixa Postal 116, 12600-970, São José dos Campos, SP, Brazil
[c] Universidade Estadual Paulista Julio de Mesquita Filho, FEG/UNESP, Av. Ariberto Pereira da Cunha, 333, 12516-410, Guaratinguetá, SP, Brazil
[d] Departamento de Ciência e Tecnologia da Aeronáutica, IAE/DCTA, Praca Marechal Eduardo Gomes, 50, 12228-904, São José dos Campos, SP, Brazil

ARTICLE INFO

Article history:
Received 28 April 2012
Accepted in revised form 13 April 2013
Available online 20 April 2013

Keywords:
Titanium alloys
Tribological properties
Powder metallurgy

ABSTRACT

Although titanium and its alloys own good mechanical properties and excellent corrosion resistance, these materials present poor tribological properties for specific applications that require wear resistance. In order to produce wear-resistant surfaces, this work is aimed at achieving improvement of wear characteristics in Ti–Si–B alloys by means of high temperature nitrogen plasma immersion ion implantation (PIII). These alloys were produced by powder metallurgy using high energy ball milling and hot pressing. Scanning electron microscopy (SEM) and X-ray diffraction identified the presence of α-titanium, Ti_6Si_2B, Ti_5Si_3, TiB and Ti_3Si phases. Wear tests were carried out with a ball-on-disk tribometer to evaluate the friction coefficient and wear rate in treated and untreated samples. The worn profiles were measured by visible light microscopy and examined by SEM in order to determine the wear rates and wear mechanisms. Ti–7.5Si–22.5B alloy presented the highest wear resistance amongst the untreated alloys produced in this work. High temperature PIII was effective to reduce the wear rate and friction coefficient of all the Ti–Si–B sintered alloys.

1. Introduction

Titanium and its alloys are extensively used in aerospace and automotive industries [1], marine structures [2,3], biomedical and sport equipments and other consumer goods [4,5]. In medical applications, some of these alloys offer high strength and excellent corrosion resistance for use in hip and knee prostheses, dental implants and orthopedic applications [6]. However, one important requirement for Ti alloys when exposed to harsh environments, as is the case in many aerospace applications [1], is the necessity to present superior tribological properties. As an example, the widely used Ti–6Al–4V alloy presents a maximum working temperature of only 500 °C and poor tribological properties [5]. In addition, the high cost of such commercial alloys has hampered the widespread use of this alloy, mainly in non-aerospace fields. In order to overcome such constraints powder metallurgy seems to be a suitable alternative process [7–9]. This solid-state process has the advantage of suppressing limitations imposed by phase diagrams [10]. Another advantage of this technique is that it is simple and economically viable when compared to other conventional processing such as arc melting.

Different hard-coatings technologies such as introducing alloying elements in coatings based on borides of transition metals via powder metallurgy have been studied to improve the wear resistance of Ti alloys [11]. Silicon added in some compositions, for example, decreases the surface roughness and increases electrical resistance and hardness while nitrogen provides high hardness [12,13]. Ti–B–N films show a lower friction coefficient and are more corrosion resistant than TiN films [14]. Ti–Si–B materials can work in high temperatures presenting good wear properties and superior resistance against oxidation [15]. Additionally, other variations (Ti–B, Ti–Mo–Si–B, Ti–Cr–Si–B, etc.) are under analysis to be used as hard-coatings [11].

Even though powder metallurgy brings about innumerous possibilities to produce a variety of alloys with low cost and special properties, a concern lays on contamination, which can occur in ball milling by particle incorporation from the milling tools and the air. Such impurity incorporation, generally increases hardness and modifies the thermodynamics of the process. Then, it is essential to use high purity starting powders to control or minimize contamination [10,16–21].

In this paper, we report about the modified tribological properties of Ti–Si–B samples, prepared by powder metallurgy, and treated by the process of plasma immersion ion implantation (PIII).

PIII showed to be very effective to improving the surface hardness and wear rate in steels and Ti–6Al–4V samples [22–25], while

* Corresponding author. Tel.: +55 12 3028 6715; fax: +55 12 3028 6710.
E-mail address: brunobacci@yahoo.com.br (B.B. Fernandes).

0257-8972/$ – see front matter © 2013 Elsevier B.V. All rights reserved.
http://dx.doi.org/10.1016/j.surfcoat.2013.04.029

preserving the properties of the bulk of these materials. For industrial applications, the tools and components treated by PIII usually present a significant increase in their lifetime [23]. Nevertheless, the main constraint for extensive use of conventional PIII is the thin modified layer, of the order of few hundred nanometers. Actually, when the material is used in harsh environments, thicker treated layers are demanded. In order to overcome this limitation, PIII must be performed under high temperature to enhance the thermal diffusion of the implanted species. The innovative high temperature PIII (HTPIII) process used to treat the Ti–Si–B samples in the current experiments is well described elsewhere [26].

In this work, friction coefficient of Ti–Si–B powder alloy samples which were treated by HTPIII are compared to the untreated ones. In addition, wear mechanisms were determined and characterized by scanning electron microscopy (SEM)/energy dispersive spectroscopy (EDS). The structure and morphology of the surfaces were also characterized by X-ray diffraction (XRD) and optical profilometry, respectively.

2. Experimental procedures

High-purity elemental powders were used in this work to prepare the following powder mixtures: Ti–7.5Si–22.5B, Ti–16Si–4B and Ti–18Si–6B (at.%). The purity, morphology and average size of the starting powders are: Ti (99.9 wt.%, spherical, <150 mesh), Si (99.999 wt.%, irregular, <325 mesh) and B (99.5 wt.%, angular, <325 mesh). The as-milled powders were handled under an argon atmosphere in a glove box system. The milling process was carried out at room temperature in a Fritsch planetary ball mill under argon atmosphere using rotary speed of 300 rpm, a ball-to-powder weight ratio of 10:1 and stainless steel vials (0.225 m^3) and balls. Balls with different diameters were used for each mixture and Table 1 shows these and other different variables adopted in milling. The milling performed under argon atmosphere is named of dry milling in such Table, and the milling in alcohol medium that was used to yield the stuck powders is denominated wet milling.

The mechanically alloyed powders were uniaxially pressed during 2 min (120 s) at 110 MPa (0.112 kgf/m^2) and isostatically pressed with 300 MPa (0.306 kgf/m^2), both operations at room temperature. The obtained green compacts were hot-pressed into graphite die under an argon atmosphere with 30 MPa (0.031 kgf/m^2) and with the conditions described in the Table 2.

The Ti–18Si–6B pellet was also sintered under vacuum by using a pressureless sintering after hot pressing. Heating rate of 20 °C/min was applied to reach sintering temperature of 1200 °C for 30 min (1800 s). The samples were grounded on SiC papers and polished with colloidal silica suspension.

HTPIII is performed in a stainless steel vacuum chamber, in a nitrogen atmosphere with a working pressure of 10^{-3} Torr. Samples of Ti–Si–B were mounted on a stainless steel rod that plays the role of the anode of the plasma glow discharge, being positively polarized by DC voltages in the 700 V range with respect to the grounded chamber wall. A thermionic oxide cathode generates primary electrons that help with the breakdown of the glow discharge and are also drawn to the samples causing them to heat, until to reach a temperature of about 800 °C. When high negative voltage pulses are applied to the samples, nitrogen ion implantation takes place. PIII was carried out with the following process parameters: high voltage pulses of 7 kV, 30 μs and 400 Hz, for 60 min (3600 s). Details of the experimental apparatus used to perform this kind of HTPIII experiment can be found in the work published by Oliveira et al. [26].

Table 2
Hot pressing conditions.

Hot pressing condition	Sintering temperature (ºC)	Heating rate (ºC/min)	Dwell time (min)	Sample compositions
(1)	1030	20	20	Ti–18Si–6B(1); Ti–7.5Si–22.5B and Ti–16Si–4B
(2)	900	20	40	Ti–18Si–6B(2)

XRD measurements were obtained by a Philips diffractometer (model PW3719 with CuKα radiation) in the standard 2θ mode (voltage of 40 kV and current of 45 mA). The structures of the samples were characterized using SEM, where compositional analysis was carried out by the EDS coupled to the device. Surface morphology of the samples was analyzed by AFM and optical profilometry (Veeco).

Measurements of dry friction coefficient were accomplished in a ball-on-disk tribometer from CSM Instruments. Parameters used were: load of 1 N (0.102 kgf) with a 3-mm diameter alumina ball as a counterpart material, linear speed of 5 cm/s (0.05 m/s) and track radius of 3 mm. The worn-out surfaces of treated and untreated samples were examined by SEM in the secondary electron mode to find out the wear mechanisms. Disk volume loss and wear rate were calculated according to equations in the ASTM G-99 [27]. Roughness and wear profiles were measured by a profilometer. Visible light microscopy was also used for the measurement of track widths.

3. Results and discussion

XRD patterns of the powder mixtures without milling present Ti, Si and B intense peaks, rather than in the as-milled mixtures – results not shown here. Such as-milled powders after only 1 hour of processing do not present B peaks and the Si peaks almost disappeared, with exception of the Ti–16Si–4B mixture in which both Si and B peaks disappeared. It is important to notice that the Ti peaks had their intensity reduced and were broadened after this period for all mixtures [28].

Previous SEM analyses of as-milled powders [28] showed particles with very coarse sizes (up to 1 mm) and with irregular morphology. However, the Ti–7.5Si–22.5B powders processed in wet milling present an *in situ* forming of particle with sizes less than 200 μm and flake shapes [29].

XRD patterns of the main region from Ti–Si–B sintered powders are presented in Fig. 1. It was found that all materials (pristine and treated samples) were mainly composed of five phases: α-titanium, Ti_6Si_2B, Ti_5Si_3, TiB and Ti_3Si. For the Ti–18Si–6B compositions, the peak intensity of Ti increased slightly after pressureless sintering. However, the intensity of Ti_3Si was reduced, suggesting dissolution of this phase into new phases, which is a consequence of the high sintering temperature (1200 °C) that is above the stability temperature of the Ti_3Si. The Ti–16Si–4B alloy presents almost the desired phases, but some Ti_3Si and TiB are found due the low hot pressing temperature

Table 1
Sample composition and milling conditions.

Sample composition	Time/interruption	Time in dry milling (h)	Time in wet milling (h)	Balls- Quantity (unit)/Dimension (mm)
Ti–7.5Si–22.5B	10 min in milling/1 min stopped	1.00	0.33	12/12; 6/16; 6/19
Ti–18Si–6B(1)		1.00	0.00	12/12; 8/16; 6/18; 40/3
Ti–18Si–6B(2)		1.00	0.00	12/12; 6/16; 6/19
Ti–16Si–4B		1.00	0.00	12/12; 8/16; 6/18

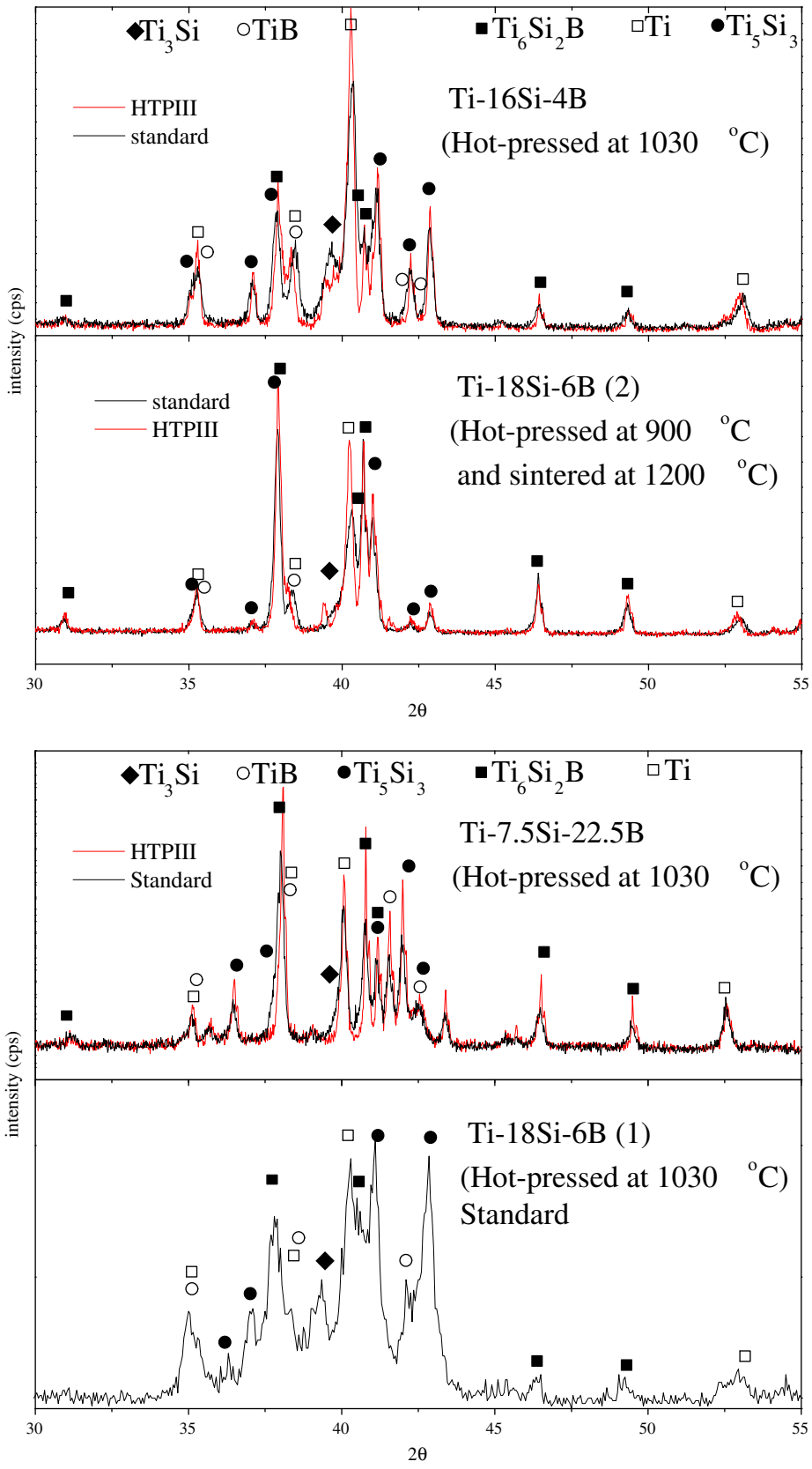

Fig. 1. XRD patterns of HTPIII treated and untreated alloys.

(1030 °C) and contamination. TiB formation on the Ti–7.5Si–22.5B was also hampered probably due to the same reasons previously stated, besides the short milling time. XRD shows a peak near the main peak of titanium for treated samples, probably due to the presence of a rich nitrogen layer. Glow discharge optical spectroscopy has been performed on Ti–6Al–4V treated with similar conditions,

and a layer of 2 μm in depth was formed [25]. As it was registered almost none modification in the XRD patterns in the present work, a layer with such depth must be also formed.

The surface topography of untreated and treated samples was identified by optical profilometry technique. Ti–16Si–4B and Ti–18Si–6B surfaces have similar morphology, presenting high heterogeneity and roughness (110 ± 30 nm). However, the Ti–7.5Si–22.5B alloy shows a more homogeneous morphology and lower roughness (52 ± 18 nm) when compared with the other compositions. After HTPIII, roughness of the silicon-rich powder alloys is raised to more than 150 nm (160 ± 33 nm – Ti–16Si–4B; 210 ± 25 nm – Ti–18Si–6B) and the Ti–7.5Si–22.5B alloy do not present significant changing on this feature (48 ± 10 nm).

The Ti_{SS} phase can be identified through SEM (Fig. 2) at the brightest areas, which is obviously located at the grain regions originating from external areas of the particles. Such phase dissolves around 7% of iron, 1% of silicon, 2% of nickel and 1% of chromium (at.%) for all compositions studied here, however the Ti–7.5Si–22.5B alloy presents a higher contamination (8%-iron, 7%-nickel). EDS analysis also indicated that the α-Ti and TiB phases dissolve around 2% (at.%) of silicon. The dark gray phase corresponds to the phases Ti_5Si_3 and Ti_6Si_2B, which has a slight difference of atomic weight making it difficult their distinction.

Nitrogen was detected by EDS in α-Ti and Ti_{SS}, but not in the silicides and borides. These new phases can also be noticed with AFM measurements that show protuberances in the surface with similar morphologies. SEM/EDS analyses of cross section samples identified a layer of TiN with approximately 700 nm.

SEM images and density measurements (Table 3) revealed that very dense alloys with maximum grain size of 60 μm were obtained. The density was around 3.6 g/cm^3 before sintering of the Ti–18Si–6B(2)

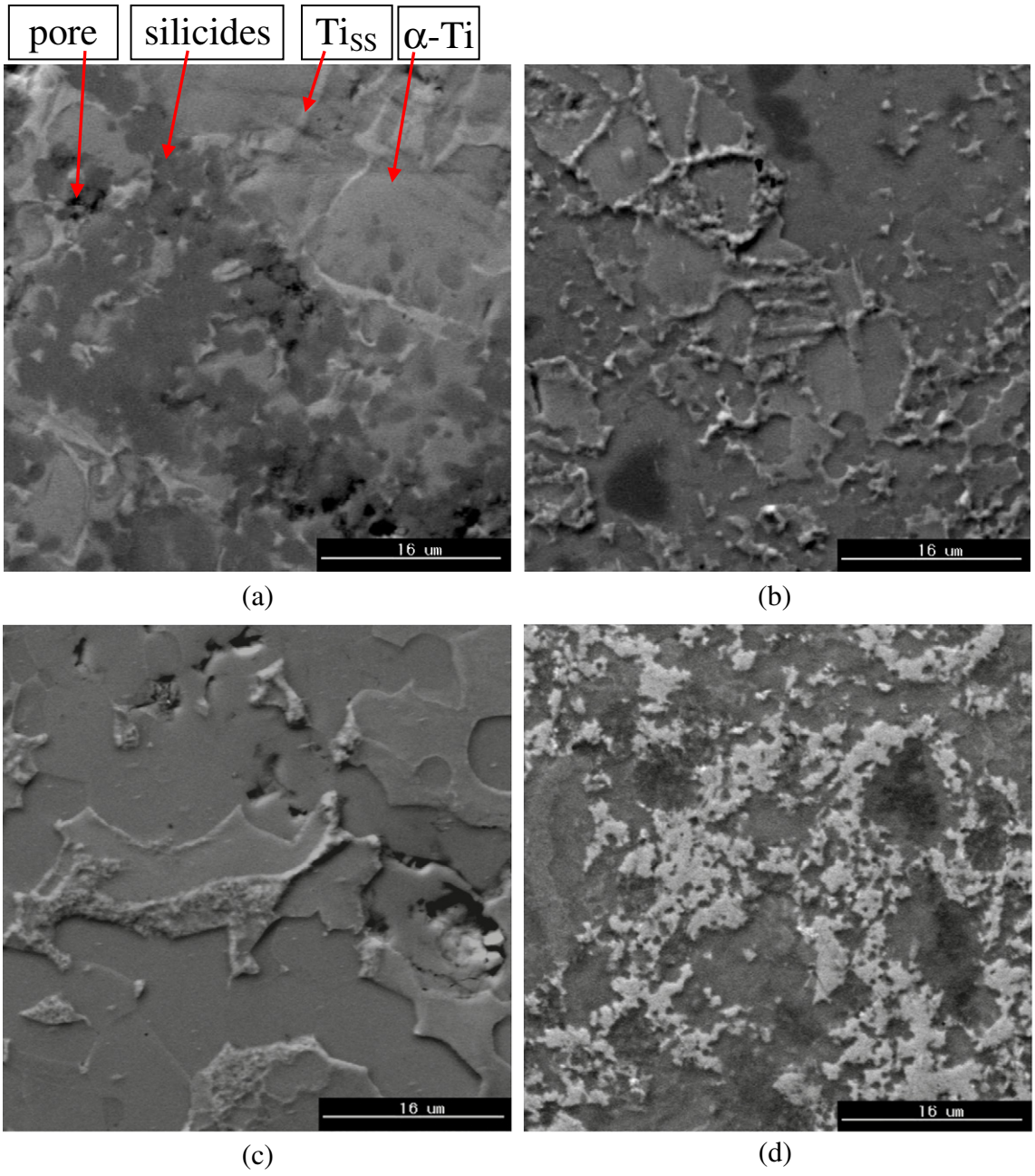

Fig. 2. SEM micrographs comparing the treated and untreated microstructures using back-scattering electrons: (a, b) Ti–16Si–4B; (c) Ti–18Si–6B(2); and (d) Ti–7.5Si–22.5B. (a) untreated, (b, c, d) treated by HTPIII.

Table 3
Densities and wear rates.

Sample composition	Measured density (g/cm^3)	Theoretical density (g/cm^3)	Wear rate ($mm^3/N\ m$)	
			Untreated	Treated
Ti–18Si–6B(1)	4.4	4.4	0.10	0.03
Ti–18Si–6B(2)	4.3	4.4	0.11	0.02
Ti–7.5Si–22.5B	4.4	4.5	0.03	0.02
Ti–16Si–4B	4.3	4.4	0.08	0.02

alloy, which also generates grain growth. It could be inferred the occurrence of a full densification of such alloys, but with the presence of contamination by heavy atoms (iron, nickel and chromium) from the milling tools and the presence of pores observed by microscopy analysis.

Fig. 3 shows the friction coefficient (CoF) curves for all studied Ti–Si–B alloys, which present significant decrease in their values after HTPIII treatment. The pristine Ti–16Si–4B sintered alloy showed an increase in CoF of 1.5 times compared with the standard Ti–6Al–4V alloy [24]. However, after HTPIII, CoF and wear rate were significantly reduced. Also, the Ti–18Si–6B(2) sintered alloy shows a high reduction in CoF and wear rate after treatment compared to the untreated sample. Ti–6Al–4V commercial alloy was tested at the same conditions that the Ti–Si–B sintered alloys. All Ti–Si–B composition without HTPIII have lower wear rates that this commercial alloy.

Pristine silicon-rich alloys presented wear mechanisms similar to Ti–16Si–4B powder alloy [30]. Fig. 4 shows the worn-out surface for untreated Ti–7.5Si–22.5B sample after wear tests. This alloy presents significant less adhesive and abrasive scars when compared with silicon-rich samples previously reported [30].This may be caused by the higher TiB content on its microstructure, which is the compound with higher hardness in these alloys.

After treatment of the surfaces by HTPIII, the resultant tracks are significantly reduced, and only few abrasive wear scars are observed by SEM operating in the secondary electrons mode (Fig. 5).

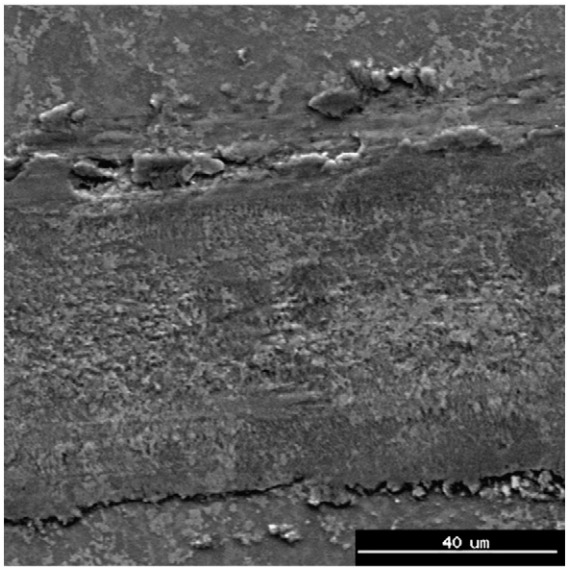

Fig. 4. Untreated Ti–7.5Si–22.5B wear scar.

4. Conclusions

Distinct Ti–Si–B alloys produced by powder metallurgy were treated by HTPIII. This plasma treatment successfully improved tribological properties of all Ti–Si–B samples by reducing their friction coefficient and/or lowering their wear rates.

XRD analyses revealed the presence of α-Ti, Ti_6Si_2B, Ti_5Si_3, TiB, Ti_3Si and TiN phases. GDOS experiments of HTPIII treated Ti–6Al–4V suggest the formation of a 2-μm layer with nitrogen. SEM/EDS analyses show a layer of TiN with about of 700 nm at the surface of the Ti–Si–B sintered alloys. However more extensive characterization by glancing incidence XRD and Auger electron spectroscopy are demanded to verify

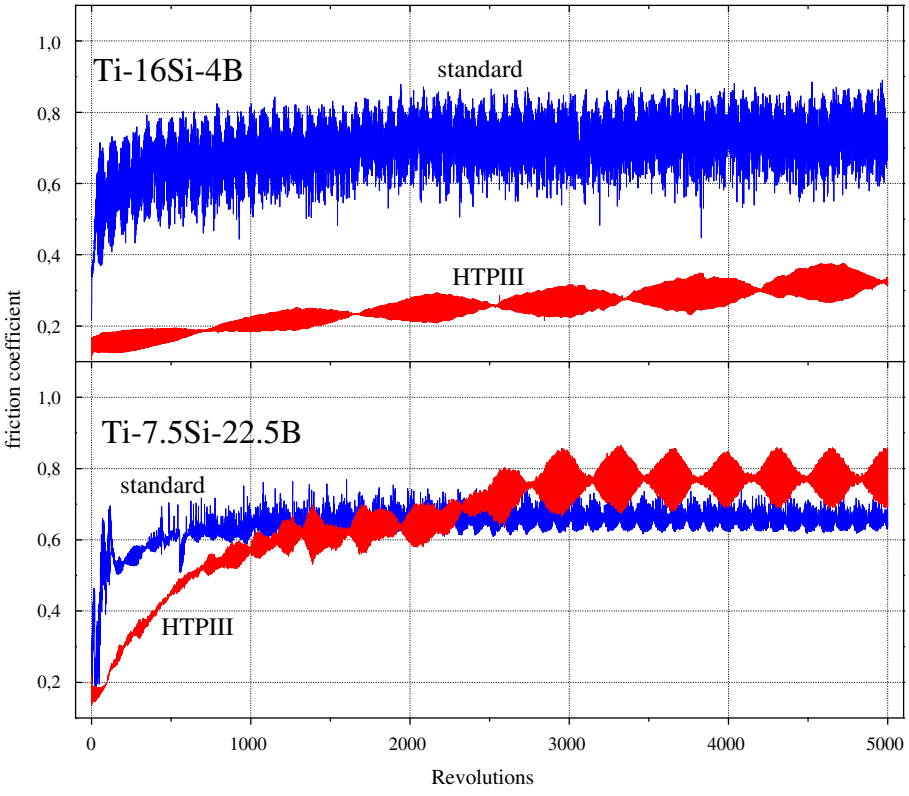

Fig. 3. Curves of friction coefficient (CoF) versus sliding revolutions for the untreated and treated Ti–Si–B samples.

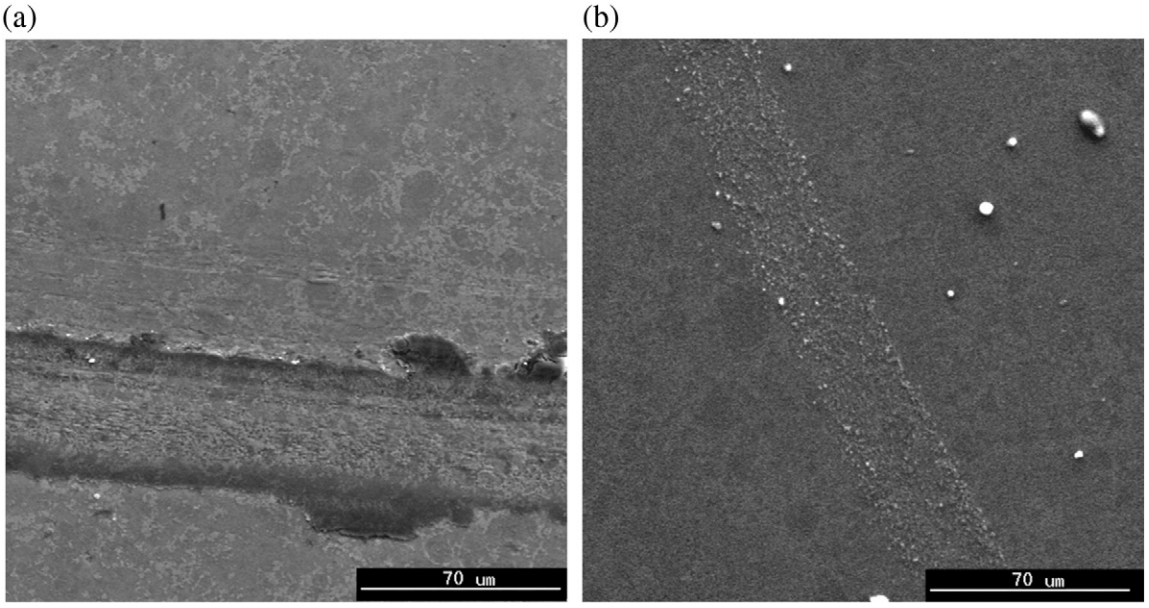

Fig. 5. SEM micrographs comparing the treated and untreated tracks using secondary electrons: (a) untreated Ti–7.5Si–22.5B; (b) treated Ti–7.5Si–22.5B.

the surface gradation of these phases. Optical profilometry results indicated a change in the roughness of the samples due to that formation of nitrogen-rich films.

Among pristine samples, the ones with Ti–7.5Si–22.5B composition presented the lowest wear rates. Nevertheless, after HTPIII, all alloys presented similar reduced wear rates, despite the differences on the CoF's, which must be better evaluated in subsequent work.

Acknowledgments

This project is partially supported by *CNPq*, *FAPESP* and *MCT*, from Brazil. The authors would like to thank Dr. C. B. Mello for some of the friction tests, Dr. V. A. H. Rodrigues for the hot pressing, Dr. C. A. A. Cairo for important information about processing parameters on powder metallurgy, M. L. Brison for the SEM data, R. R. Cunha for some of the XRD measurements, Dr. J. P. B. Machado for optical profilometry, M. M. N. F. Silva for support on HTPIII treatments and several co-workers from *ITA*, *IAE* and *INPE*.

References

[1] M. Yamada, Mater. Sci. Eng., A 213 (1996) 8.
[2] I.V. Gorynin, Mater. Sci. Eng., A 263 (1999) 112.
[3] I. Gurrappa, Mater. Charact. 51 (2003) 131.
[4] A. Zhecheva, W. Sha, S. Malinov, A. Long, Surf. Coat. Technol. 200 (2005) 2192.
[5] G. Lütjering, J.C. Williams, Titanium: Engineering Materials and Process, 2nd ed. Springer-Verlag, Berlin Heidelberg, 2007. 442.
[6] K. Wang, Mater. Sci. Eng., A 213 (1996) 134.
[7] F.H. Froes, D. Eylon, Int. Mater. Rev. 35 (1990) 162.
[8] T. Fujita, A. Ogawa, C. Ouchi, H. Tajima, Mater. Sci. Eng., A 213 (1996) 148.
[9] Y. Liu, L.F. Chen, H.P. Tang, C.T. Liu, B. Liu, B.Y. Huang, Mater. Sci. Eng., A 418 (2006) 25.
[10] C. Suryanarayana, E. Ivanov, V.V. Boldyrev, Mater. Sci. Eng., A 304–306 (2001) 151.
[11] G.W. Stachowiak, A.W. Batchelor, Engineering Tribology, 3rd ed. Elsevier, Butterworth Heinemann, 2005. 419.
[12] D.V. Shtansky, A.N. Sheveiko, M.I. Petrzhik, F.V. Kiryukhantsev-Korneev, E.A. Levashov, A. Leyland, A.L. Yerokhin, A. Matthews, Surf. Coat. Technol. 200 (2005) 208.
[13] D.V. Shtansky, E.A. Levashov, A.N. Sheveiko, J.J. Moore, J. Mater. Synth. Process. 6 (1) (1998) 61.
[14] M. Tamura, H. Kubo, Surf. Coat. Technol. 54/55 (1) (1992) 255.
[15] E.C.T. Ramos, G. Silva, A.S. Ramos, C.A. Nunes, C.A.R.P. Baptista, Mater. Sci. Eng., A 363 (2003) 297.
[16] G. Zhang, P.A. Blenkinsop, M.L.H. Wise, Intermetallics 4 (1996) 447.
[17] B.S. Murty, M. Mohan Rao, S. Ranganathan, Acta Metall. Mater. 43 (1995) 2443.
[18] P. Bhattacharya, P. Bellon, R.S. Averback, S.J. Hales, J. Alloys Compd. 368 (2004) 187.
[19] C.J. Lu, J. Zhang, Z.Q. Li, J. Alloys Compd. 381 (2004) 278.
[20] P.J. Counihan, A. Crawford, N.N. Thadhani, Mater. Sci. Eng., A 267 (1999) 26.
[21] O.M. Ivasishin, D.G. Savvakin, F. Froes, V.C. Mokson, K.A. Bondareva, Powder Metall. Met. Ceram. 41 (7–8) (2002) 382.
[22] In: A. Anders (Ed.), Handbook of Plasma Immersion Ion Implantation and Deposition, John Wiley and Sons Inc., Montreal, 2000, p. 55.
[23] M. Ueda, L.A. Berni, R.M. Castro, Surf. Coat. Technol. 200 (2005) 517.
[24] C.B. Mello, M. Ueda, M.M. Silva, H. Reuther, L. Pichon, C.M. Lepienski, Wear 267 (2009) 867.
[25] R.M. Oliveira, C.B. Mello, G. Silva, J.A.N. Gonçalves, M. Ueda, L. Pichon, Surf. Coat. Technol. 205 (2011) S111.
[26] R.M. Oliveira, J.A.N. Gonçalves, M. Ueda, J.O. Rossi, P.N. Rizzo, Surf. Coat. Technol. 204 (2010) 3009.
[27] G-99 Standard Test Method for Wear Testing with a Pin-on-Disk Apparatus in ASTM Standards, 2000.
[28] B.B. Fernandes, Technological Institute of Aeronautics, São José dos Campos, Brazil, 2010. , (Doctorate Thesis).
[29] G. Oliveira, S.F.M. Mariano, B.B. Fernandes, M. Ueda, A.S. Ramos, Mater. Sci. Forum 727–728 (2012) 287.
[30] B.B. Fernandes, M. Ueda, C.B. Mello, P.B. Fernandes, H. Reuther, A.S. Ramos, Intermetallics 19 (2011) 693.